Pergamon

www.elsevier.com/locate/jaerosci

PII: S0021-8502(99)00534-0

J. Aerosol Sci. Vol. 31, No. 1, pp. 121–136, 2000

Printed in Great Britain
0021-8502/99/$ - see front matter

PREPARATION OF ZnS NANOPARTICLES BY ELECTROSPRAY PYROLYSIS

I. Wuled Lenggoro,* Kikuo Okuyama,*† Juan Fernández de la Mora‡ and Noboru Tohge§

* Department of Chemical Engineering, Hiroshima University, Higashi-Hiroshima 739-8527, Japan
‡ Department of Mechanical Engineering, Yale University, New Haven, CT 06520-2159, U.S.A.
§ Department of Metallurgical Engineering, Kinki University, Higashi-Osaka 577-0818, Japan

(*First received* 6 *October* 1997; *and in final form* 23 *June* 1998)

Abstract—Zinc sulfide particles 20–40 nm in diameter were prepared by electrically driven spray pyrolysis. Solutions of ethyl alcohol with zinc nitrate ($Zn(NO_3)_2$) and thiourea ($SC(NH_2)_2$) at concentrations from 0.0025 to 0.2 mol l^{-1} and electrical conductivities between 10^{-4} and 10^{-1} S m^{-1} were electrosprayed from steady cone-jets at flow rates from 0.05 to 0.16 ml h^{-1}, with positive and negative polarity. The initially highly charged drops formed were neutralized by bipolar ions from a radioactive source to increase the overall transmission efficiency through a reactor furnace. This process was made particularly effective by the innovation of placing the ion source directly within the electrospray chamber. The diameters of the final ZnS particles were measured on-line by a differential mobility analyzer and a condensation nucleus counter. In spite of ambiguities in the flow rate of liquid through the cone–jet (associated to solvent evaporation from the meniscus), these diameters agree approximately with values expected from available scaling laws. Transmission electron micrographs also confirmed these results. Electrospray pyrolysis is hence able to generate non-agglomerated and spherical ZnS nanoparticles with geometrical standard deviation σ_g of about 1.3. © 1999 Elsevier Science Ltd. All rights reserved

1. INTRODUCTION

Spray-pyrolysis is a droplet-to-particle conversion process, whose low cost and simplicity has stimulated its frequent use in the preparation of a variety of functional material particles and thin films (Gurav *et al*., 1993; Messing *et al*., 1993). In this technique, aqueous solutions of metal salts are first atomized into droplets, which are subsequently pyrolyzed to become solid particles. The average diameter of the final solid particles can be roughly determined from the droplet size and the solute concentration of the solution sprayed. The atomizers most commonly used to generate such droplets (twin-fluid or ultrasonic nebulizers) tend to produce average diameters in the range of several microns. For a droplet to dry from a typical initial diameter of 5 μm into a particle with a diameter of 0.1 μm, the initial volume fraction of dissolved involatile solute must be less than 0.0008%. In practice, these low solution concentrations lead to a low particle generation rate and make it difficult to maintain a high purity of the final particle product. In spite of these difficulties, Okuyama *et al*. (1997) have produced size-controlled zinc sulfide (ZnS) and cadmium sulfide (CdS) particles by changing the solution concentrations in ultrasonic spray pyrolysis. Their ultrasonic nebulizer generated droplets 4.56 μm in average diameter, from which ZnS and CdS particles 0.2–1.5 μm were prepared by varying the solution concentrations from 0.001 to 0.3 mol l^{-1}. However, as noted by Rulison and Flagan (1994a), the preparation of particles below 0.1 μm via traditional spray pyrolysis methods remains problematic.

The electrospray technique is one of the few known schemes capable of atomizing a liquid into ultrafine droplets. In this method, the meniscus of a conducting solution supported at the end of a capillary tube becomes conical when charged to a high voltage (several KV) with respect to a counter electrode. Droplets are then formed by the continuous breakup of a steady jet naturally forming at the apex of this cone, generally called a "Taylor cone" (Taylor, 1964). The full structure is often referred to as a cone–jet (Cloupeau and

† Author to whom correspondence should be addressed.

Prunet-Foch, 1994). A variety of experimental studies have shown that the diameter of such jets and drops may be controlled from nanometers in liquid metals (Benassayag *et al.*, 1995) up to hundreds of micrometers in dielectric liquids such as heptane (Jones and Thong, 1971), mostly through the electrical conductivity of the liquid or the flow rate (e.g., Smith, 1986; Rossel-Llompart and Fernández de la Mora, 1994; Ganan-Calvo *et al.*, 1997). Recently, Chen *et al.* (1995) have reported the production of approximately monodisperse dry residues in the range of 40 nm to 1.8 μm using aqueous sucrose solutions with electrical conductivities ranging from 1.56×10^{-3} to 8×10^{-1} S m^{-1}. This work has been extended by Chen and Pui (1997) to a variety of other liquids with dielectric constants from 12.5 to 182.

The droplets generated in an electrospray are always highly charged. Their associated large electrical mobility hence leads to considerable losses by deposition onto the walls, which decreases drastically the particle overall throughput efficiency. This difficulty is compounded by the occurrence of Rayleigh disintegration during the drying process, which broadens the initial narrow size distribution. Fortunately, these two problems may be eliminated by neutralizing the drops immediately after production. Electrical neutralizations of electrosprayed droplets through a source of ions of the opposite polarity has been reported among others by Noakes *et al.* (1989), Meester *et al.* (1993) and Chen and Gomez (1996). Cloupeau (1994) reviewed four possible neutralization methods; a unipolar-type corona discharge, an electrospray of a volatile liquid, thermoelectric emission, and a flame. Recently, the application of a radioactive bipolar ion source as the neutralizer for electrospray drops was reported by Zarrin *et al.* (1991a, b), Lewis *et al.* (1994), Chen *et al.* (1995) and Kaufman *et al.* (1996) with two Po-210 sources (370 MBq) and by Rulison and Flagan (1994b) with one Po-210 source (185 MBq).

Following the pioneering work of Fenn and his colleagues, the most common use of electrosprays has been as ion sources for mass spectrometry of large and labile biomolecules (Fenn *et al.*, 1989). However, there have been a wide variety of other applications of electrosprays in particle production (e.g., Bollini *et al.*, 1975; Mahoney *et al.*, 1987; Levi *et al.*, 1988; Salata *et al.*, 1994; Danek *et al.*, 1994, 1996; Jensen and Sorensen, 1996; Reneker and Chun, 1996; Hull *et al.*, 1997; Sobota and Sorensen, 1997; Teng *et al.*, 1997), including spray pyrolysis (Slamovich and Lange, 1990; Park and Burlitch, 1992; Rulison and Flagan, 1994a). A preliminary study of Okuyama *et al.* (1996) has also reported the production of ZnS and CdS particles below 0.1 μm in diameter by electrospray pyrolysis. However, in none of these earlier studies on electrospray pyrolysis was the spray functioning mode fully determined as a function of spray liquid flow rate or applied voltage, nor were the precise influences of the concentration or the physical properties of the solutions on the size of generated solid particles entirely clarified.

The present work constitutes the first attempt at a systematic control of all the key variables governing electrospray pyrolysis, including liquid flow rate, applied voltage and solute concentration, while operating in the steady cone–jet mode (Cloupeau and Prunet-Foch, 1989, 1990). The particles generated are measured on-line by a differential mobility analyzer and a condensation nucleus counter system, as well as off-line by thermophoretic sampling followed by transmission electron micrographic analysis. In spite of ambiguities regarding the actual liquid flow carried by the jet (due to solvent evaporation from the meniscus), the particle sizes determined after drying compare favorably with those expected from available scaling laws for the original drops.

2. EXPERIMENTAL APPARATUS AND PROCEDURE

Figure 1 shows the set-up used to generate ZnS particles and investigate the effect of experimental conditions on their physical characteristics. It comprises (i) an electrospray source, (ii) a reaction furnace, and (iii) a size-analysis section, including a differential mobility analyzer (DMA, TSI model 3071), a condensation nucleus counter (CNC, TSI model 3020), and a home-made thermophoretic sampler.

Earlier studies on the preparation of ZnS and CdS particles using ultrasonic spray pyrolysis have used pure water as the solvent. However, because of its large surface tension,

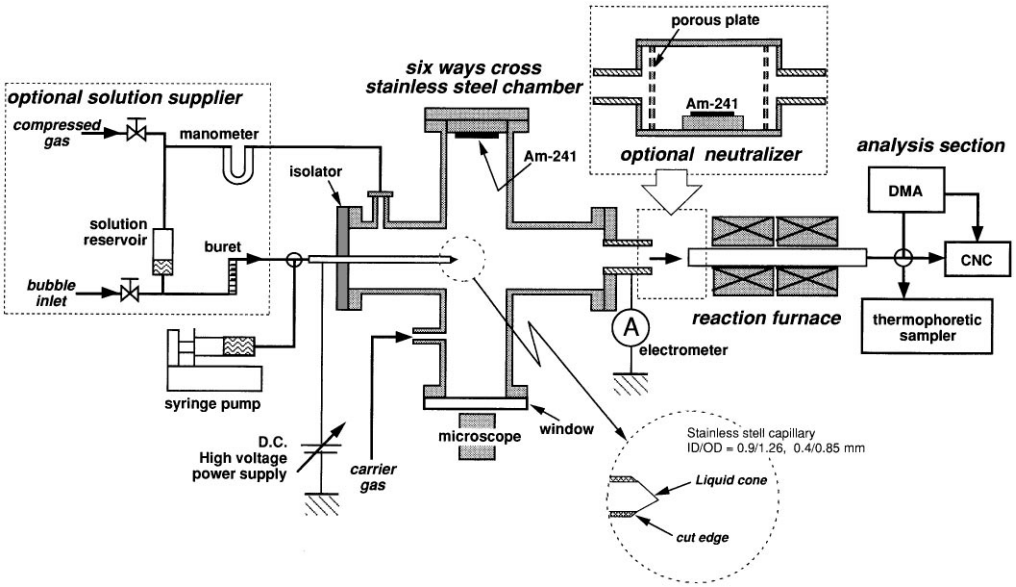

Fig. 1. Schematic of the overall experimental apparatus of electrospray pyrolysis.

establishment of a Taylor cone of water requires high applied voltages that leads to electrical breakdown of the surrounding air. In the positive mode, this difficulty may be overcome by using a sheath gas with relatively high electrical breakdown threshold, such as CO_2 or SF_6 (Zeleny, 1915; Smith, 1986). However, because CO_2 would lead to oxidation of the Zn in the final product, we have used nitrogen as a sheath gas, at a constant flow rate of $1.0\,l\,min^{-1}$. Zinc nitrate [$Zn(NO_3)_2$] and thiourea [$SC(NH_2)_2$] were used as the sources of Zn and S, respectively. Ethanol was chosen as the solvent because of its good solubility in these two solutes, as well as for its low surface tension, which makes it possible to produce stable Taylor cones of positive and negative polarity in nitrogen.

As described in equation (1) (Tohge and Minami, 1992), zinc nitrate and thiourea form a complex in solution. The droplets containing the complex are then pyrolyzed to synthesize directly ZnS particles at a furnace temperature around 600°C which is necessary to drive the reaction (Okuyama *et al.*, 1997).

$$Zn(NO_3)_2 + (NH_2)_2SC \Rightarrow Zn(SC(NH_2)_2)_2(NO_3)_2 \Rightarrow ZnS. \quad (1)$$

The molar ratio of Zn : S was kept constant at 1 : 2, since pure ZnS phase could not be obtained at 1 : 1 (Zn : S). This behavior has been observed in previous work by Tohge and his colleagues on the formation of ZnS particles via spray pyrolysis (Tohge *et al.*, 1995) who varied the ratio of Zn : S from 1 : 1 to 1 : 3. The crystalline phase found was hexagonal in the range of temperatures from 600 to 800°C, while higher temperature led to the appearance of ZnO phase in addition to ZnS. For reasons which remain unclear, the best and purest ZnS phase was obtained at Zn : S = 1 : 2. In another study on the preparation of CuS particles using ultrasonic spray pyrolysis, Lenggoro *et al.* (1998) found that they could not produce CuS with Cu : S = 1 : 1, the best CuS phase being formed again for Cu : S = 1 : 2. Hence, it appears that the decomposition of the dissolved complex involves the loss of sulfur, perhaps via H_2S.

Table 1 shows the physical properties of the solvent and solutions used. Four different solution concentrations C_s were electrosprayed. Increasing C_s by two decades did not change substantially the density ρ and viscosity μ of the liquid, but increased its electrical conductivity K by about 35 times (compare the highest with the lowest C_s), and by 1600 times with respect to the unseeded solvent. The most important physical property of the solution controlling both the stability of the electrospray (Cloupeau and Prunet-Foch, 1989; Tang and Gomez, 1996) and the droplet size is known to be the liquid electrical

Table 1. Physical properties of the pure solvent and the solutions used

C_s (mol l^{-1})	ρ (kg m^{-3})	μ (mPa s)	K (S m^{-1})
0	788.9	1.207	1.20×10^{-4}
0.0025	789.6	1.220	5.62×10^{-3}
0.01	791.5	1.243	2.01×10^{-2}
0.05	801.4	1.365	6.53×10^{-2}
0.20	838.8	1.822	1.92×10^{-1}

conductivity K. Thus, this study focused on this parameter. Notably, the value K around 0.2 S m^{-1} is fairly large in relation to typical literature values. The electrical conductivity of the solutions was measured by a conductivity meter (Toko Chemical Inc., TX-90) at 25°C and the liquid density and viscosity by an Ostwald-type pycnometer and a viscometer, respectively.

The liquid was sprayed inside a six ways cross stainless-steel chamber (Fig. 1). Two of the opposing sides were used for supplying the spraying liquid and sampling the generated aerosols. Positive and negative DC high voltage sources (Matsusada Co. Ltd., HER-10R3) were connected to the stainless-steel capillaries. Two such capillaries were used, having inner/outer diameters of 0.90/1.20 and 0.40/0.88 mm. These will be referred to as the "large" and the "small" capillary, respectively. Each capillary tip was tapered conically down to nearly zero thickness. The liquid was supplied to the capillary either through a programmable syringe pump (Harvard Apparatus, Model 55) or, optionally, by introducing compressed nitrogen above the sample liquid inside a vertical syringe. In the latter method, the flow rate of solution was calibrated by measuring the moving velocity of a gas bubble injected into the solution line through a burette.

In order to reduce the evaporation of solvent at the cone, an attempt was made to saturate the nitrogen gas with ethanol vapor by passing it through an ethanol reservoir. A precipitate, however, still appeared at the capillary tip after running times of tens of minutes at solution concentrations ranging from 0.05 to 0.2 mol l^{-1}.

A stainless-steel tube having an inner diameter of 5 mm was used to sample the aerosol. Its distance to the spraying needle was adjustable, but was kept at 40 mm for most runs. This sampling tube was grounded through an electrometer (Keithley, model 485) for measuring the electric current brought by the droplets that were deposited onto it and the chamber wall. This allowed monitoring the stability of the electrospray. The noise level of the electrometer remained in the range of 1.0 nA. The spray capillary electrode and sampling tube were set horizontally to facilitate the connection of the spray chamber to a furnace or a DMA-CNC system. Another pair of opposite sides of the chamber are windows for monitoring the meniscus shape at the capillary tip, through a 30 × microscope set at one side and a continuous light source at the other.

Because of its simplicity and stability, an α-ray radioactive source (^{241}Am; 2.22 MBq) was used to produce bipolar ions for drop neutralization. It was placed several millimeters in front of the conical tip in the axial direction, and about 45 mm in the radial direction, above the range of the α-rays from ^{241}Am (40 mm). To test the effectiveness of the neutralizer, the number concentration of the generated particles was measured right at the outlet of the spray chamber. It increased from a value of the order of 10^2 or 10^3 without neutralization up to 10^6 particles cm^{-3} with neutralization. This favorable tendency was also observed when the ^{241}Am was located at the outlet of the spray chamber, as described in Fig. 1. Since neutralization of the particles could greatly improve their throughput efficiency, the ^{241}Am source was installed in all subsequent experiments.

The neutralization scheme used in this work differs from all other approaches which we are aware of in that the ion source is not electrically shielded from the high fields created by the spraying needle. Earlier work on the combustion of electrosprayed drops of fuel (Thong and Weinberg, 1971; see also Chen and Gomez, 1996) isolated flame chemi-ions from the spraying needle by means of a grounded metal gauge. Similarly, Kaufman and colleagues

and Rulison and Flagan have introduced their radioactive source in a chamber downstream from the electrospray chamber. Presumably, these precautions were inspired by the well-known fact that the physical situation is quite different when the gas surrounding the meniscus ceases to be a perfect insulator. For instance, dating back to Zeleny's early observations, there are numerous reports showing that discharges originating at the tip of the cone do modify the stability range of the cone–jet, the current-flow rate relation, and most likely also the diameter of the emitted drops. Even in the presence of a peculiarly weak and visually imperceptible discharge sometimes arising for water electrosprays in air change to CO_2, Tang and Gomez (1995) have reported that the corresponding stability island is extended considerably towards smaller flow rates, while the drop diameter corresponding to a given flow rate is smaller than in the pure cone–jet mode. In spite of these precedents, we find that the current versus voltage relations are not shifted in any substantial way by the presence or absence of the radioactive source, provided that it is kept more than 40 mm away from the needle. Hence, it is clear that electrical isolation of the cone–jet from the ion source is not always essential, at least when the space charge in the spray region consumes a sufficient fraction of the ions to avoid an excessive disturbance of the usual dynamics of the Taylor cone. It is worth noticing that, although the neutralization scheme of Rulison and Flagan (1994b) was inspired in TSI's approach (Zarrin *et al*., 1991), the relatively large aperture they introduced between the electrospray and the neutralizer chamber allowed partial penetration of the field from the needle into the chamber containing bipolar ions, and some of these were clearly drawn into the region of the needle, as indicated by the authors remark "With no spray established, gas ions generated some current when an electric field was applied. On the other hand, with a spray established, the current was the same with and without the discharger. This indicates that the ions were probably intercepted by liquid droplets". Note, however, that the current was measured with a modest resolution of only 10 nA.

Besides its greater simplicity, two advantages of introducing the neutralizer directly into the electrospray chamber are that: (i) drop losses associated to the passage from the electrospray region to the neutralization region are avoided, and (ii) neutralization is more immediate, with a consequently reduced danger of Coulombic explosions.

The droplets generated were introduced from the spray chamber into a reaction furnace using nitrogen carrier gas. In order to reduce the loss of particles, a relatively short tubular furnace was used. It comprised a quartz glass tube of 20 mm inner diameter and 200 mm long, with two independently controlled heating zones 10 cm long. The residence time inside the furnace was estimated to be 1.5 s for $1.0\,l\,min^{-1}$ of carrier gas flow. All experiments were made at atmospheric pressure and with a furnace temperature of 600°C.

Following the heated furnace, the resulting dry ZnS particles were sized with a DMA-CNC system, similarly as in earlier studies. The sheath air in the DMA is set to $10\,l\,min^{-1}$ and the flow ratio of aerosol to sheath air is kept at 0.1. Alternatively, a thermophoretic sampler with a 150-mesh brass grid was placed at the outlet of the furnace. These samples were examined and photographed by transmission electron microscopy (TEM) to verify and support the data obtained from the DMA-CNC system.

3. EXPERIMENTAL RESULTS

3.1. *Determination of the stability domain of the cone–jet*

Different spray modes may lead to quite different drop size distributions for a given solution (e.g. Cloupeau and Prunet-Foch, 1989). Hence, before measuring the particle size distributions, one must distinguish and control the regime at which the liquid cone and the spray operate. Figure 2 shows typical curves of the electric current versus the applied voltage of (a) ethanol and (b) $0.0025\,mol\,l^{-1}$ solution, performed without the ^{241}Am neutralizer using the apparatus shown in Fig. 1. Flow rates fed to the small capillary by a syringe pump were kept constant at (a) $0.20\,ml\,h^{-1}$ and (b) $0.08\,ml\,h^{-1}$. First, the applied positive voltage was increased gradually, and then reduced after the liquid meniscus at the

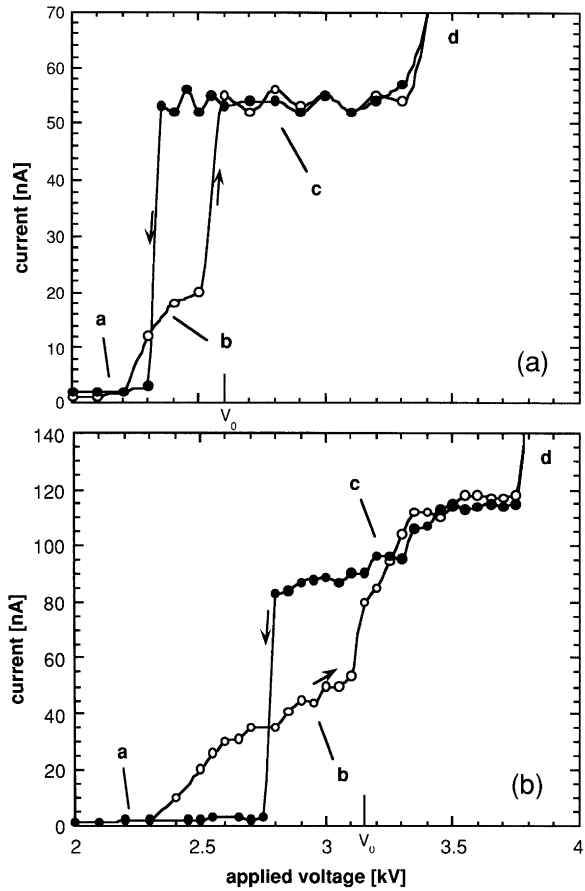

Fig. 2. Typical current versus applied voltage curve of ethanol (a) and 0.0025 mol l^{-1} solution (b). Characters a, b, c, d indicate the formation of different liquid meniscus as described in Fig. 3. Flow rates Q were 0.20 (a) and 0.08 ml h^{-1} (b). The measurements were performed with the small capillary and at positive applied voltage, without a neutralizer (^{241}Am), and using the apparatus shown in Fig. 1.

capillary tip passed some spray modes. When the applied voltage increased from a small initial absolute value (Fig. 2a), the liquid on the capillary tip was changed from a meniscus to a dripping mode (Fig. 3a). Increases in the frequency of the dripping and the current were observed with increasing applied voltage, leading eventually to the so-called pulsating mode (Fig. 3b), where the meniscus shape alternates between a cusp and a hemisphere. Increasing the voltage further increases the pulsating frequency, until, at a critical voltage, the liquid meniscus forms a stable Taylor cone (Fig. 3c) and the current jumps drastically.

When increasing the voltage at constant liquid flow rate, the volume of the liquid cone decreased, and the cone angle increased. At a second and higher critical voltage, the current and the meniscus became unstable, and multiple jets appeared at the tip of the capillary (Fig. 3d). In the reverse way, the operating mode of the liquid meniscus (the cone) evolved similarly as under increasing voltage, but with a hysteresis loop in the appearance of the cone–jet mode. Figure 2 is globally similar to that depicted on the voltage–current characteristic reported in other papers (Smith, 1986; Chen *et al.*, 1995).

For a given solution concentration C_s, a stable cone–jet may be established only within a certain domain of flow rates Q and applied voltage V, $Q_{min}(V) < Q < Q_{max}(V)$ (Cloupeau and Prunet-Foch, 1989), Q_{min} and Q_{max} being the corresponding minimum and maximum flow rates. This stable domain is affected by C_s (electrical conductivity K), shifting toward smaller flow rates as C_s increases.

The inner diameter of the capillary was seen to affect the stability domain of the cone–jet. Cloupeau and Prunet-Foch (1989) and Tang and Gomez (1996) have reported a similar

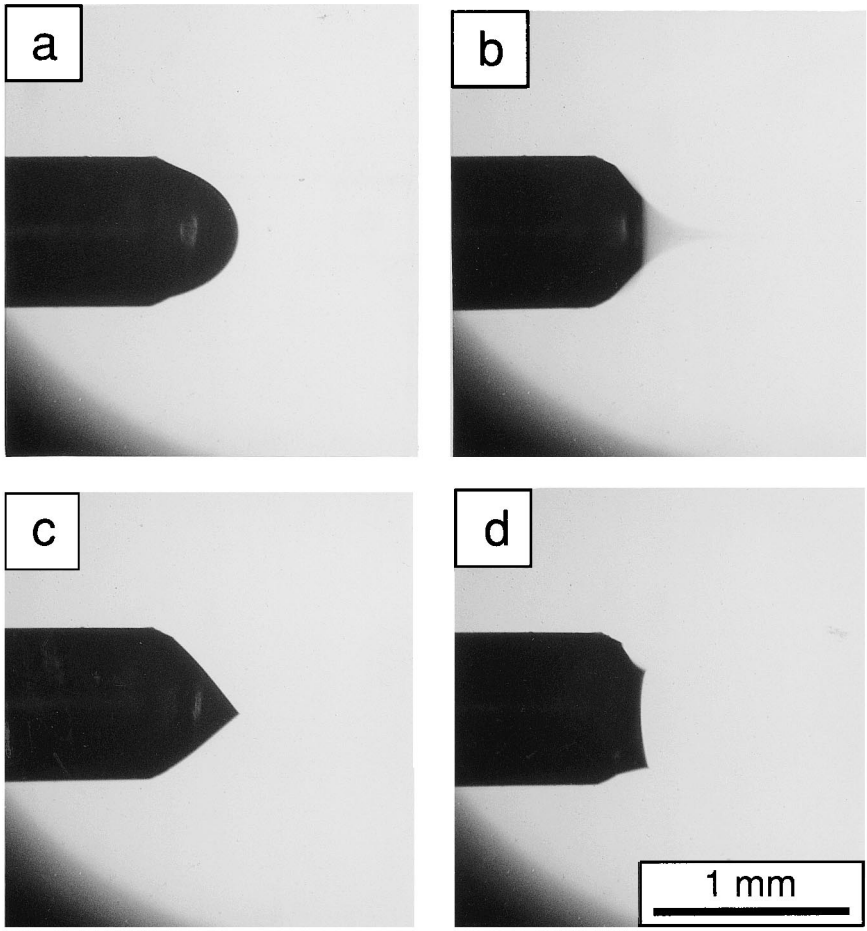

Fig. 3. Photographs of the various meniscus shapes: (a) dripping mode, (b) pulsating mode, (c) stable cone–jet mode, and (d) multi-jet mode.

behavior for the different case of liquids with low dielectric constant and low conductivity, with Q_{min} increasing as the capillary diameter increases. However, most other studies with conducting liquids observed no effect of either the electrostatic variables or the capillary diameter on Q_{min} (Fernández de la Mora, 1992; Fernández de la Mora and Loscertales, 1994; Rossel-Llompart and Fernández de la Mora, 1994; Chen *et al*., 1996, 1997; Ganan-Calvo *et al*., 1997). The unusual trend found here is surely due to the fact that the evaporation flux Q_{evap} of liquid from the meniscus is not negligible at the scale of the relatively small flow rates involved in this work, particularly at the higher electrical conductivities. If we define Q_{jet} as the liquid flow rate Q pushed through the jet, and Q_{feed} as that fed to the capillary, mass conservation implies that $Q_{jet} = Q_{feed} - Q_{evap}$. For given Q_{jet}, Q_{evap} is larger for the larger capillary, hence requiring that Q_{feed} be also larger than for the small capillary. Consequently, the use of a large capillary causes a narrowing of the cone–jet domain of the electrospray. This observation is in consonance with the fact that the spray current is independent of the applied voltage in Fig. 2a (low conductivity), but increases with it in Fig. 2b (high conductivity). In the first case, $Q_{evap} \ll Q_{feed}$, and there is no dependence on electrostatic variables, as discussed in earlier work. The behavior in Fig. 2b may be explained by the reduction of the cone angle (hence the area available to evaporation) with cone voltage, which then gives rise to an increase in Q_{jet} which itself increases the spray current.

The sign of the applied voltage was also found to affect the stable cone–jet domain, negative voltages requiring higher flow rates (both Q_{min} and Q_{max}) than positive voltages.

However, this effect is most likely due to the appearance of corona discharges, favored in the negative mode (Zeleny, 1915), and frequently observed visually in this work.

At the higher C_s, the first mode to appear is occasionally the cone–jet mode (Cloupeau and Prunet-Foch, 1994). As mentioned before, at $C_s = 0.05$ and particularly at 0.2 mol l^{-1}, the salt precipitated on the capillary tip after several tens of minutes of operation, even when the carrier gas was saturated with ethanol. This made the sampling of the particles difficult, since more than 1 h is needed to obtain a suitable quantity of sample.

Due to the volatility problem and other differences (electrode geometry, liquid properties such as electrical conductivity and vapor pressure), the range of liquid flow rates where we could form a stable spray was narrower in this work than in earlier studies (Rossel-Llompart and Fernández de la Mora, 1994; Cloupeau and Prunet-Foch, 1989; Chen *et al.*, 1995). For instance, in the case of $C_s = 0.0025$ mol l^{-1} spraying at small capillary and positive voltage, Q_{min} was 0.09 and Q_{max} was about 0.20 ml h^{-1}. The narrowest range, i.e. the smallest ratio Q_{max}/Q_{min} was found at $C_s = 0.2$ mol l^{-1}, with $Q_{min} = 0.05$ ml h^{-1} and $Q_{max} = 0.08$ ml h^{-1}. No stable spray could be formed at any voltage in our system below 0.05 ml h^{-1}.

Since it has been previously established that lower flow rates of spray liquids generate smaller and more narrowly dispersed electrospray droplets (Rossel-Llompart and Fernández de la Mora, 1994), an attempt was made in this study to maintain Q near the minimum value Q_{min}. At a certain applied voltage $V(Q)$, we find that the cone is most easily controlled near Q_{min}, where the fluctuation of the current is also smallest.

3.2. *Size distribution of ZnS particles*

Particle size distributions were measured using a DMA–CNC system. In each case, the furnace temperature was kept at 600°C and the liquid flow rate Q was near or at the minimum value Q_{min}. Figure 4 shows the influence of the applied (negative) voltage and the electrospray mode on the particle size distributions for $C_s = 0.01$ mol l^{-1} and $Q = 0.10$ ml h^{-1}. The particle size distribution function expressed by $f(\ln d_p)$ is

$$f(\ln d_p) = (\Delta n/\Delta \ln (d_p))/N, \tag{2}$$

and the data were relaxed following Adachi *et al.* (1990). Δn is the number concentration in the size range Δd_p, and N is the total particle number concentration. All the figures show a geometrical standard deviation σ_g of about 1.3. Figure 4a corresponds to the pulsating mode, with an associated volume mean diameter d_p of 32.6 nm. The particle size distributions for the cone–jet modes are shown in Fig. 4b (3.15 and 3.5 kV). This corresponds to finer particles than in the pulsating mode, where the oscillation between two different meniscus shapes and the related formation of a transient jet introduces different and larger breakup volumes (Cloupeau and Prunet-Foch, 1989, 1990; Chen *et al.*, 1995).

Figure 4b shows aerosol size distributions for the cone–jet mode, indicating that the volume mean diameter increases slightly with increasing applied voltage. A similar tendency was reported by Rulison and Flagan (1994b). Tang and Gomez (1996) find an analogous trend in electrosprays of heptane, although the behavior of such low conductivity liquids is known to be quite different from that of our own solvent. On the other hand, Rossel-Llompart and Fernández de la Mora (1994) as well as Chen *et al.* (1995, 1997) find that droplet size is nearly independent of applied voltage for liquids of high electrical conductivity. Again, the discrepancy with our results and with those of Rulison and Flagan (1994b; who used a capillary diameter of 1.65 mm for solution conductivities between 0.007 and 0.356 S m^{-1}) is probably due to solvent evaporation from the meniscus, since a higher voltage reduces the cone volume and hence the evaporation loss. An indication of the evaporation problem experienced by Rulison and Flagan (1994b) is given by their anomalously high liquid flow rates. On page 138 they note a disagreement by factors ranging from 30 and 80 betwen their jet radius a and the formula $a \sim [\rho Q^2/(2\gamma\pi^2)]^{1/3}$ proposed by Fernandez de la Mora *et al.* Indeed, this relation was later shown to be approximately valid only at relatively large flow rates, but not near the minimum value (Rossel-Llompart and

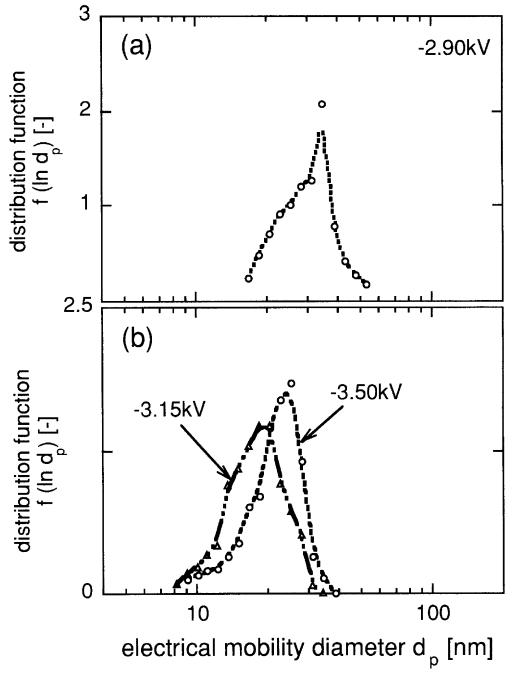

Fig. 4. Measured particle size distributions at (a) pulsating mode (2.90 kV) and (b) stable cone–jet mode: 3.15 and 3.50 kV, for a solution concentration $C_s = 0.01$ mol l^{-1} and a flow rate of 0.06 ml h^{-1}.

Fernández de la Mora, 1994). However, the error involved is proportional to the factor $\eta^{2/3}$ introduced later in equation (6), which is always of order unity near the minimum flow rate. The disagreement factors of 30–80 reported are hence more likely due to substantial errors in Q associated to liquid evaporation. This problem is clearly present also in Fig. 5 of Rulison and Flagan (1994a), which plots the liquid flow rate versus electrical conductivity under fixed conditions of the jet geometry. Although the scaling laws now firmly established (see Section 4.2) require that the product KQ be constant, their figure shows that Q asymptotes towards a relatively large constant value as K increases. The asymptote corresponds most likely to the rate of liquid evaporation from the meniscus. The evaporation problem hence remains in their work as well as in ours, in spite of their efforts to saturate the carrier gas with solvent vapor.

Figures 5 and 6 show the size distributions of particles generated in the cone–jet mode from the small capillary, at various concentration of spray solutions C_s, and at positive and negative voltages, respectively. All of the cases show that varying C_s has almost no influence on the volume mean diameter in the distributions, which remains in the range from 20 to 30 nm. The particle size distributions found with the large capillary (not shown) also indicate an insensitivity of the size distribution to the solution concentration. In contrast, Rulison and Flagan (1994b) reported that more concentrated solutions made smaller solid particles. These differences will be discussed in Section 4.

Although available scaling laws for the cone–jet indicate that the drop diameter should show little dependence on the sign of the needle voltage (in the absence of discharges), the present study constitutes the first direct measurement (and comparison) of size distributions obtained with both polarities.

3.3. *Photographs of ZnS particles*

The ZnS particles prepared earlier by ultrasonic spray pyrolysis were somewhat dense and spherical and had a smooth surface (Tohge *et al.*, 1996). Figure 7 shows TEM photographs of ZnS particles electrosprayed from the small capillary, under positive

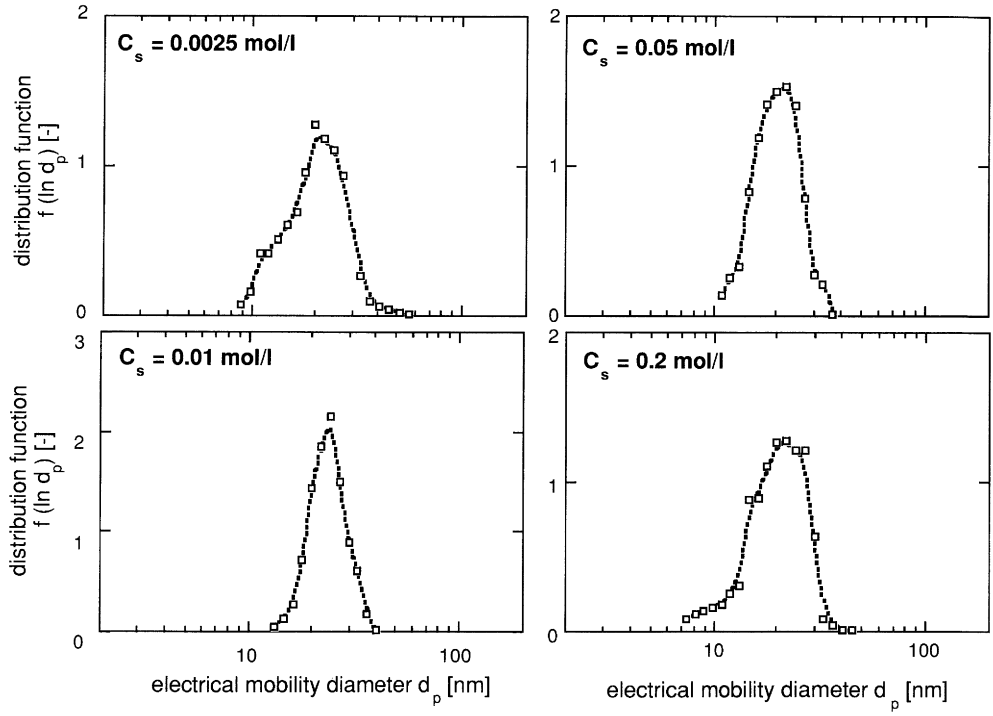

Fig. 5. Measured particle size distributions at various solution concentration C_s (mol l^{-1}). The flow rates were set near the minimum value at each C_s. Small capillary; positive needle voltage.

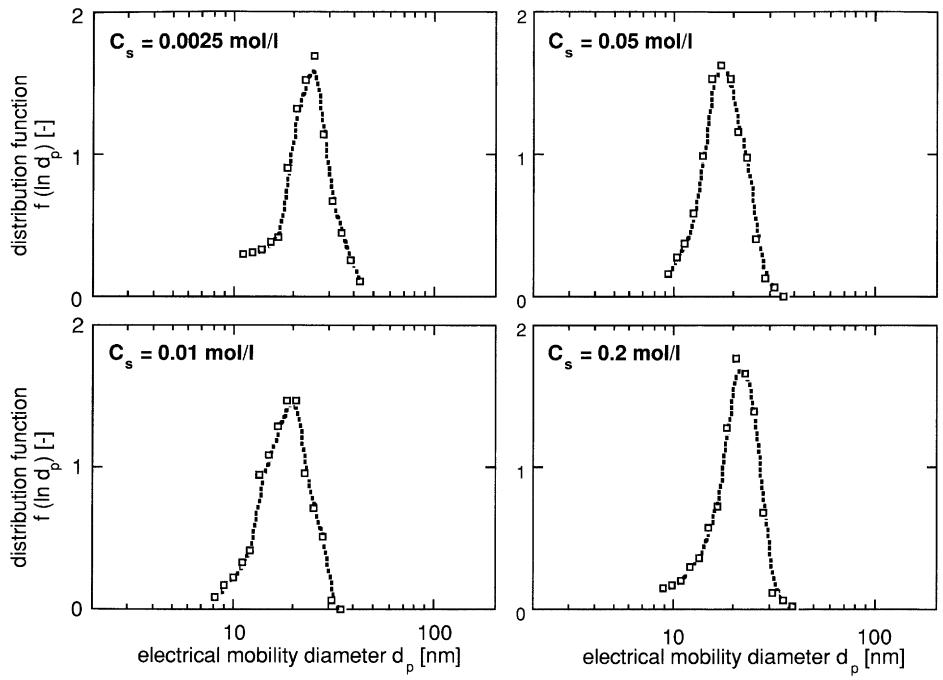

Fig. 6. Measured particle size distributions at various solution concentration C_s (mol l^{-1}). The flow rates were set near the minimum value at each C_s. Small capillary; negative voltage.

polarity, from a solution concentration of 0.01 mol l^{-1} and at a flow rate of 0.10 ml h^{-1}. The shapes of the particles are spherical, with size distributions similar to those of Fig. 5. Comparable TEM photographs (not shown) were obtained when varying other parameters such as the capillary size, the sign of the applied voltage, and the solution concentrations.

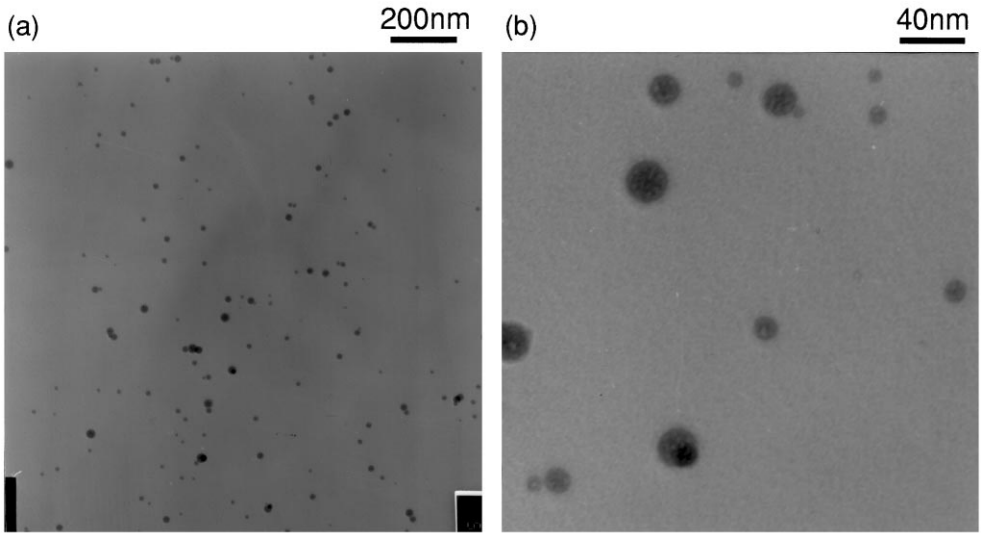

Fig. 7. TEM photographs of ZnS particles collected over a period of 2 h from electrosprayed solutions. $C_s = 0.01$; flow rate = 0.06 ml h^{-1}. The magnification is 50,000× in (a) and 250,000× in (b).

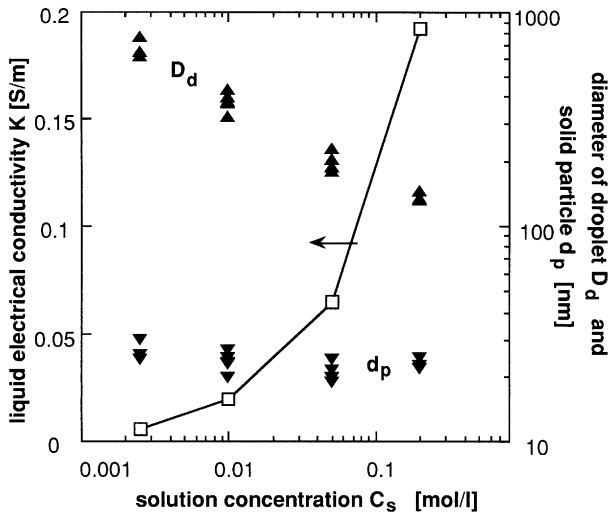

Fig. 8. Measured volume mean particle diameter d_p from the size distribution, and associated droplet diameter D_d [from equation (3b)] as a function of solution concentration C_s. The electrical conductivities K are shown also as open squares.

The TEM study confirmed the mobility diameter data measured by the DMA-CNC combination.

4. DISCUSSION

4.1. *Prediction of droplet diameter*

Figure 8 shows the relation between the volume mean particle diameter d_p, the electrical conductivity of the solution K, and the volume mean droplet diameter D_d as functions of solution concentration C_s. d_p was inferred from the distributions of mobility diameter found earlier with the DMA–CNC system in the cone–jet mode (Figs 4–6). The droplet diameter D_d was predicted using equation (3a), derived from the mass balance between the droplet

and the final solid particle d_p under the assumption that each drop turned into a dense spherical particle, without disruption during the spray pyrolysis.

$$d_p^3 = (MD_d^3C_s)/1000\rho, \tag{3a}$$

where M and ρ are the molecular weight and the bulk density of solid ZnS, and C_s is the solution concentration in $\mathrm{mol\,l^{-1}}$. For ZnS with $M = 97.46$ and $\rho = 4.09\ \mathrm{g\,cm^{-3}}$ equation (3a) can be written as

$$d_p = 0.288 D_d C_s^{1/3}. \tag{3b}$$

Figure 8 shows a strong dependence of the droplet diameter on the electrical conductivity K of the spray solution. The volume mean droplet diameter D_d ranged from 140 to 580 nm, and decreased with increasing K. The increased solution concentration led to dry particles whose size was a larger fraction of the initial droplet size. But it also increased K, which resulted in smaller droplet sizes. In this study, the overall result of these two factors was a solid particle size in a narrow range of 20–30 nm, independent of K.

4.2. *Size evaluation of droplet and particle based on scaling laws*

The scaling laws found in the studies of Fernández de la Mora and Loscertales (1994), Rossel-Llompart and Fernández de la Mora (1994), Chen *et al.* (1995), Ganan-Calvo *et al.* (1997) and Chen and Pui (1997) can be used to evaluate the size of the droplets generated in our system. These earlier investigations found that the droplet diameters are nearly independent of external electrostatic variables (electrode geometry and voltage), depending mostly on flow rate and liquid properties. When the flow rate ratio Q/Q_{min} takes values not too large (typically smaller than 16), Rossel-Llompart and Fernández de la Mora (1994) find that the droplets form mainly in a single size, whose initial diameter D_d^* scales with the electrical relaxation length r^* defined in equation (4a). The following equations can be given for the case of polar liquid with electrical permittivity $\varepsilon > 6$ (see also de Juan and Fernandez de la Mora, 1997 and Ganan-Calvo *et al.*, 1997) and electrical conductivity K typically larger than $10^{-5}\ \mathrm{S\,m^{-1}}$.

$$D_d^* = G(\varepsilon) r^*, \tag{4a}$$

$$r^* = (Q\varepsilon\varepsilon_o/K)^{1/3}, \tag{4b}$$

where Q is the flow rate pushed through the jet and ε_o is the electrical permittivity of vacuum. Available data on G compiled from the literature are shown in Table 2. G depends mainly on ε, but is also influenced by the following viscosity variable (Rossel-Llompart and Fernández de la Mora, 1994):

$$\Pi(\mu) = (\rho\gamma^2\varepsilon\varepsilon_o/K)^{1/3}/\mu, \tag{5}$$

where γ is the surface tension of the liquid. $\Pi(\mu)$ accounts for viscous effect on the jet breakup, which increases the ratio between the diameter of the drops and that of the jet. In particular, the diameter of "satellite" droplets made dimensionless with r^* depends steeply on $\Pi(\mu)$ at values of this parameter below 0.06, but seems to level off for $\Pi(\mu) > 0.15$. Table 3 shows that $\Pi(\mu)$ ranges between 0.4 and 2 for the present solutions, for which only slight viscous effects should be expected.

The electrical permittivity ε and the surface tension γ were not measured, and these solution properties have been assumed to be equal to those of pure ethanol ($\gamma = 0.02275\ \mathrm{N\,m^{-1}}$; $\varepsilon = 24.3$). $G(\varepsilon)$ also appeared to be a constant, independent of the dimensionless flow rate parameter η,

$$\eta = [\rho Q K/(\gamma\varepsilon\varepsilon_o)]^{1/2}. \tag{6}$$

At the highest solution concentrations ($C_s = 0.05$ and $0.2\ \mathrm{mol\,l^{-1}}$) the smallest values of η were as large as 15 ± 2 and 24 ± 3 (Table 3), several times larger than the values $\eta_{min} \sim 1$

Table 2. Values of $G(\varepsilon)$ [equation (4)] drawn from the literature

Sources	ε	$G(\varepsilon)$	Note
Fernández de la Mora and Loscertales (1994)	~ 40	0.76	*1
Rossel-Llompart and Fernández de la Mora (1994)	20	0.68	*2
Aguirre-de-Carcer and Fernández de la Mora (1995)	80	0.60–1.10	*3
de Juan and Fernández de la Mora (1997)	81	0.648	*4
Chen and Pui (1997)	12.5–182	1.23–0.70	*5

Note:
*1 Supported by optical determination of jet diameters.
*2 Based on aerodynamics measurements of droplet diameter.
*3 Dd of water have been obtained by a phase Doppler anemometry.
*4 Droplets of water in a wide range of K, rearranged the data of Chen *et al.* (1995).
*5 Fitted function $G(\varepsilon) = -10.87\varepsilon^{-6/5} + 4.08\varepsilon^{-1/3}$ (water and ethylene glycol solutions).

Table 3. Characteristic of the initial drops electrosprayed (small capillary, positive polarity)

C_s (mol l^{-1})	Q (ml h^{-1})	d_p (nm)	D_d (nm)	η —	Π —	r^* (nm)	D_d^* (nm) ($G = 0.60$)	D_d^* (nm) ($G = 0.75$)
0.0025	0.10	22.8	583.6	5.02	2.050	1021.0	612.6	765.8
0.01	0.07	21.9	353.1	7.95	1.317	592.6	355.6	444.5
0.05	0.06	23.4	220.7	13.35	0.813	380.1	228.1	285.1
0.20	0.05	23.8	141.6	21.38	0.432	249.7	149.8	187.3

found in previous studies for polar liquids. This anomaly is also most probably due to considerable evaporation in our meniscus. Had we been able to attain smaller flow rates and hence produced smaller drops at given K, we should have been able to find a decrease in the final particle size at increasing K. This is in fact what was seen by Rulison and Flagan, whose evaporative loss problem hence appears to have been milder than ours.

For the present purposes, considering the value of ε to be 24.3, G was assumed to be between 0.60 and 0.75. Table 3 shows also the calculated data obtained from the experimental conditions described in Fig. 5 for the particular case of the small capillary and positive polarity. The values of D_d given by equation (3) agree best with D_d^* calculated by the scaling laws [equation (4)] when $G(\varepsilon)$ is 0.60.

The experimental data in points of Fig. 9a and b are replotted from Fig. 8. The error bars do not account for ambiguities in either the value of $G(\varepsilon)$ (fixed at 0.60 in all calculations of D_d^*), the liquid flow rate (we used Q_{feed} rather than Q_{jet}) or its electrical conductivity (we used K_{feed} rather than K_{jet}). They are associated to the experimental size scatter found at a given solution concentration, the lower bound corresponding to the smaller size observed when using the small capillary, and the higher bound to the maximum size measured with the large capillary. The values of the solid particle diameter used are volume mean diameters. The scaling law predicts initial drop diameters in the ranges of 665 ± 50 nm for the case of $C_s = 0.0025$ mol l^{-1}, and 163 ± 13 nm for the case of $C_s = 0.2$ mol l^{-1}. The resulting volume mean particle diameters were predicted to be between 20 and 30 nm.

Evaporation modifies the predicted initial drop diameter, not only by making $Q_{jet} < Q_{feed}$, but also by increasing the solution concentration near the cone tip. Hence, the local value of the electrical conductivity increases, so that $K_{jet} > K_{feed}$. Both effects may be comparable in magnitude in the limit when K is proportional to salt concentration. They tend to compensate each other in the prediction of the spray current, while they add to each other in the prediction of the drop diameter. The conductivity would be modified only if the salt diffusivity were sufficient to spread the salt-enriched surface layer into the interior of the meniscus. Otherwise, C_s would increase only in a narrow outer liquid layer, where the salt would be greatly enriched and precipitate, more in consonance with our observations at higher concentrations. We may obtain an upper estimate for the error in Q due to evaporation by comparing the observed and predicted currents while taking $K_{jet} = K_{feed}$.

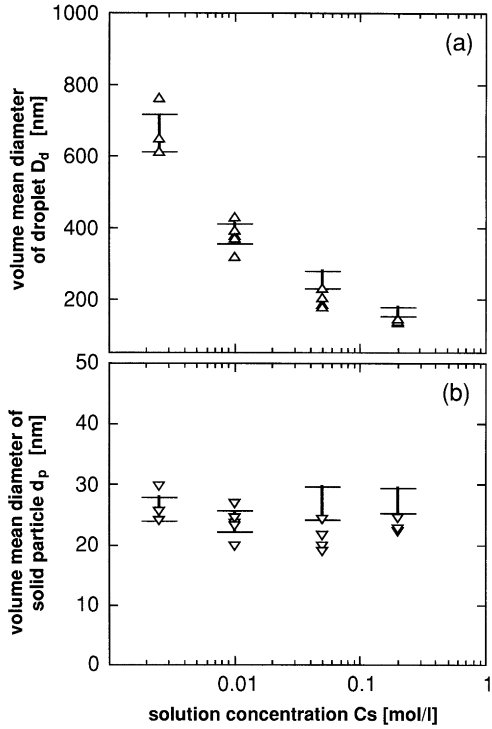

Fig. 9. Data of Fig. 8 [(a) for D_d and (b) for d_p] compared to the ranges (error bars) expected from the scaling laws [equation (4) with $G = 0.6$] for each solution concentration C_s.

It ranges from 17 to 40% for $C_s = 0.0025$ moll^{-1}, and up to 85% for $C_s = 0.2$ moll^{-1}. The corresponding droplet diameter error is much smaller because of the slow dependence (1/3 power law) of r^* on K and Q. It varies in this estimate from 5 to 11% ($C_s = 0.0025$ moll^{-1}) to around 30% ($C_s = 0.2$ moll^{-1}). Such ambiguities are by no means negligible; but they are still comparable with the scatter in the data shown in Fig. 9 as well as with the indeterminacy in the value of G. In spite of these uncertainties, Fig. 9 shows a fair agreement between predictions and observations, with only a slight overprediction at higher C_s. Hence one may produce particles of a desired size, just by controlling the physical properties of the solution and its flow rate.

The difficulties found here at higher C_s should be avoided in the future by spraying the solution from finer capillaries, where evaporation may be greatly reduced (Chen *et al.*, 1995). This precaution will also allow a wider range of flow rate variation, and hence a smaller final particle diameter. Elimination of the evaporative problem will also avoid salt precipitation and hence increase the spray stability. This will undoubtedly allow approaching the considerably narrower size distributions observed in earlier electrospray atomization, which makes us think that mean particle diameters below 10 nm with geometrical standard deviation σ_g below 1.1 should be attainable in electrospray pyrolysis.

We have seen only unimodal size distributions, perhaps because we operate near minimum flow rate. Note that at higher Q, a bifurcation phenomenon tends to occur, leading to bimodal particle size distributions (Rossel-Llompart and Fernández de la Mora, 1994; de Juan and Fernández de la Mora, 1997). Other possible reasons for the absence of smaller satellite drops from our samples is their preferential loss by deposition onto the walls, or the limitations of our measuring instrumentation. For instance, the size range of the DMA is from 5 to 200 nm, while the efficiency of the CNC is down to 50% at 5 nm.

5. CONCLUSION

The potential of the electrospray pyrolysis technique in the synthesis of nanosized zinc sulfide particles 20–40 nm in diameter has been demonstrated by on-line size

measurement with a DMA–CNC system and confirmed by TEM photographs of collected samples. Electrospray can finely atomize ethyl alcohol solutions of zinc nitrate and thiourea under a variety of experimental conditions such as: solution concentrations between 0.0025 and 0.2 mol l^{-1}; electrical conductivities between 10^{-4} and 10^{-1} S m^{-1}; liquid flow rates of about 0.10 ml h^{-1}; positive and negative needle voltages; and various capillary geometries. Neutralization of the highly charged drops initially produced with the bipolar ions from an α-ray radioactive source greatly improves the throughput efficiency of the generated particles. The measured final particle sizes are in agreement with a process where solution drops are initially electrosprayed with diameters obeying known scaling laws, and then dry into final compact and spherical particles. The smallest particle diameters generated here ($\sim$ 20 nm) and the geometrical standard deviation observed ($\sigma_g \sim 1.3$) do not represent fundamental limits of the electrospraying technique used, and could probably be improved substantially by use of narrower capillaries. The novel neutralization technique introduced should be useful in a considerably wider range of applications than those considered here.

Acknowledgment—The authors wish to thank Mr K. Hayashi (Toda Kogyo Corporation, Hiroshima) for taking the TEM photographs of the particles, as well as Prof. A. Gomez (Yale) for insights into the subject of drop neutralization. Support from the Ministry of Education, Culture and Science of Japan (Grant No. 08650893), the Hosokawa Powder Technology Foundation and the Electric Technology Research Foundation of Chugoku, is gratefully acknowledged. I.W.L. is greatly indebted to the Agency for the Assessment and Application of Technology BPPT, Indonesia, for a fellowship.

REFERENCES

Adachi, M., Okuyama, K., Kousaka, Y., Moon, S. W. and Seinfeld, J. H. (1990) Facilitated aerosol sizing using the differential mobility analyzer. *Aerosol Sci. Technol.* **12,** 225–239.

Aguirre-de-Carcer, I. and Fernández de la Mora, J. (1995) Effect of background gas on the current emitted from Taylor cones. *J. Coll. Interf. Sci.* **171,** 512–517.

Benassayag, G., Sudraud, P. and Jouffrey, B. (1985) *In situ* high voltage TEM observations of an EHD source. *Ultramicroscopy* **16,** 1–8.

Bollini, R., Sample, S. B., Seigal, S. D. and Boarman, J. W. (1975) Production of monodisperse charged metal particles by harmonic electrical spraying. *J. Coll. Interf. Sci.* **51,** 272–277.

Chen, G. and Gomez, A. (1996) Co-flow laminar diffusion flames of monodisperse sprays: structure, evaporation and microgravity effects. *Comb. Sci. Technol.* **115,** 177–202.

Chen, D. R. and Pui, D. Y. H. (1997) Experimental investigation of scaling laws for electrospraying: dielectric constant effect. *Aerosol Sci. Technol.* **27,** 367–380.

Chen, D. R., Pui, D. Y. H. and Kaufman, S. L. (1995) Electrosprays of conducting liquids for monodisperse aerosol generation in the 4 nm to 1.8 μm diameter range. *J. Aerosol Sci.* **26,** 963–977.

Cloupeau, M. (1994) Recipes for use of EHD spraying in cone–jet mode and notes on corona discharge effects. *J. Aerosol Sci.* **25,** 1143–1157.

Cloupeau, M. and Prunet-Foch, B. (1989) Electrostatic spraying of liquids in cone–jet. *J. Electrostat.* **22,** 135–159.

Cloupeau, M. and Prunet-Foch, B. (1990) Electrohydrodynamic spraying functioning of liquids in cone–jet. *J. Electrostat.* **25,** 165–184.

Cloupeau, M. and Prunet-Foch, B. (1994) Electrohydrodynamic spraying functioning modes: a critical review. *J. Aerosol Sci.* **25,** 1021–1036.

de Juan, L. and Fernández de la Mora, J. (1997) Charge and size distributions of electrospray drops. *J. Coll. Interf. Sci.* **186,** 280–293.

Danek, M., Jensen, K. F., Murray, C. B. and Bawendi, M. G. (1994a) Electrospray organometallic chemical vapor deposition—A novel technique for preparation of II–VI quantum dot composites. *Appl. Phys. Lett.* **65,** 2795–2797.

Danek, M., Jensen, K. F., Murray, C. B. and Bawendi, M. G. (1996) Synthesis of luminescent thin-film CdSe/ZnSe quantum dot composites using CdSe quantum dots passivated with an overlayer of ZnSe. *Chem. Mater.* **8,** 173–180.

Fenn, J. B., Mann, M., Meng, C. K., Wong, S. F. and Whitehouse, C. M. (1989) Electrospray ionization for mass spectrometry of large biomolecules. *Science* **246,** 64–71.

Fernández de la Mora, J. (1992) The effect of charge emission from electrified liquid cones. *J. Fluid Mech.* **243,** 561–574.

Fernández de la Mora, J. and Loscertales, I. G. (1994) The current transmitted through an electrified liquid conical meniscus. *J. Fluid Mech.* **260,** 155–184.

Ganan-Calvo, A. M., Davila, J. and Barrero, A. (1997) Current and droplet size in the electrospraying of liquids scaling laws. *J. Aerosol Sci.* **28,** 249–275.

Gurav, A., Kodas, T., Pluym, T. and Xiong, Y. (1993) Aerosol processing of materials. *Aerosol Sci. Technol.* **19,** 411–452.

Hull, P. J., Hutchison, J. L., Salata, O. V. and Dobson, P. J. (1997) Synthesis of nanometer-scale silver crystallites via a room-temperature electrostatic spraying process. *Adv. Mater.* **9,** 413–416.

Jensen, H. and Sorensen, G. (1996) Ion bombardment of nano-particle coatings. *Surf. Coatings Technol.* **84,** 500–505.

Jones, A. R. and Thong, K. C. (1971) The production of charged monodisperse fuel droplets by electrostatic dispersion. *J. Phys. D* **4,** 1159–1166.
Kaufman, S. L., Skogen, J. W., Dorman, F. D., Zarrin, F. and Lewis, K. C. (1996) Macromolecule analysis based on electrophoretic mobility in air: Globular proteins. *Anal. Chem.* **68,** 1895–1904. See also correction *Anal. Chem.* **68,** 3703 (1996).
Lenggoro, I. W., Kang, Y. C., Komiya, T., Okuyama, K. and Tohge, N. (1998) Formation of submicron copper sulfide particles using spray pyrolysis method. *Jpn. J. Appl. Phys.* **37,** L288–L290.
Levi, C. G., Jayaram, V., Valencia, J. J. and Mehrabian, R. (1988) Phase selection in electrohydrodynamic atomization of alumina. *J. Mater. Res.* **3,** 969–983.
Lewis, K. C., Dohmeier, D. M., Jorgensen, J. W., Kaufman, S. L., Zarrin, F. and Dorman, F. D. (1994) Electrospray-condensation particle counter: a molecule-counting LC detector for macromolecules. *Anal. Chem.* **66,** 2285–2292.
Mahoney, J. F., Taylor S. and Perel, J. (1987) Fine powder production using electrohydrodynamic atomization. *IEEE Trans. Ind. Appl.* **IA-23,** 197–204.
Meesters, G. M. H., Vercoulen, P. H. W., Marijnissen, J. C. M. and Scarlett, B. (1992) Generation of micron-sized droplets from the Taylor cone. *J. Aerosol Sci.* **23,** 37–49.
Meshing, G. L., Zhang, S. C. and Jayanthi, G. (1993) Ceramic powder synthesis by spray pyrolysis. *J. Am. Ceram. Soc.* **76,** 2707–2726.
Noakes, T. J., Pavey, I. D., Bray, D. and Rowe, R. C. (1989) Apparatus for producing a spray of droplets of a liquid. *U.S. Patent*, 4829996.
Okuyama, K., Lenggoro, I. W., Tagami, N., Tamaki, S. and Tohge, N. (1996) Formation of ultrafine particles of metal sulfide by electrostatic spray pyrolysis method. *J. Soc. Powder Technol. Jpn.* **33,** 192–198.
Okuyama, K., Lenggoro, I. W., Tagami, N., Tamaki, S. and Tohge, N. (1997) Preparation of ZnS and CdS fine particles with different particle sizes by a spray-pyrolysis method. *J. Mater. Sci.* **32,** 1229–1237.
Park, D. G. and Burlitch, J. M. (1992) Nanoparticles of anatase by electrostatic spraying of an alkoxide solution. *Chem. Mater.* **4,** 500–503.
Reneker, D. H. and Chun, I. (1996) Nanometre diameter fibres of polymer produced by electrospinning. *Nanotechnology* **7,** 216–223.
Rossel-Llompart, J. and Fernández de la Mora, J. (1994) Generation of monodisperse droplets 0.3 to 4 μm in diameter from electrified cone–jets of highly conducting and viscous liquids. *J. Aerosol Sci.* **25,** 1093–1120.
Rulison, A. J. and Flagan, R. C. (1994a) Electrospray atomization of electrolytic solutions. *J. Coll. Interf. Sci.* **167,** 135–145.
Rulison, A. J. and Flagan, R. C. (1994b) Synthesis of yttria powders by electrospray pyrolysis. *J. Amer. Ceram. Soc.* **77,** 3244–3250.
Salata, O. V., Dobson, P. J., Hull, P. J. and Hutchison, J. L. (1994) Fabrication of PbS nanoparticles embedded in a polymer film by a gas-aerosol reactive electrostatic deposition technique. *Adv. Mater.* **6,** 772–775.
Slamovich, E. B. and Lange, F. F. (1990) Densification behavior of single-crystal and polycrystalline spherical particles of zirconia. *J. Am. Ceram. Soc.* **73,** 3368–3375.
Smith, D. P. H. (1986) The electrohydrodynamic atomization of liquids. *IEEE Trans. Ind. Appl.* **IA-22,** 527–535.
Sobota, J. and Sorensen, G. (1997) Ion bombardment of solid lubricating nanoparticle coatings. *Nucl. Inst. Methods Phys. Res.-Sect.B- Beam Interact. Mater. Atoms* **127,** 945–948.
Tang, K. and Gomez, A. (1995) Generation of monodisperse water droplets from electrosprays in a corona-assisted cone–jet mode. *J. Coll. Interf. Sci.* **175,** 326–332.
Tang, K. and Gomez, A. (1996) Monodisperse electrosprays of low electric conductivity liquids in the cone-jet mode. *J. Coll. Interf. Sci.* **184,** 500–511.
Taylor, G. I. (1964) Disintegration of water drops in an electric field. *Proc. Roy. Soc. London* **A 280,** 383–397.
Teng, W. D., Huneiti, Z. A., Machowski, W., Evans, J. R. G., Edirisinghe, M. J. and Balachandran, W. (1997) Towards particle-by-particle deposition of ceramics using electrostatic atomization. *J. Mater. Sci. Lett.* **16,** 1017–1019.
Thong, K. C. and Weinberg, F. J. (1971) Electrical control of the combustion of solid and liquid particulate suspensions. *Proc. Roy. Soc. London* **A 324,** 201–215.
Tohge, N. and Minami, T. (1992) Formation process of Cd and Zn chalcogenide-doped glasses via gels containing thiourea or selenourea complexes. *SPIE Proc. Sol–Gel Optics II* **1758,** 587–595.
Tohge, N., Tamaki, S. and Okuyama, K. (1995) Formation of fine particles of zinc sulfide from thiourea complexes by spray-pyrolysis. *Jpn. J. Appl. Phys.* **34-2,** L207–L209.
Zarrin, F., Kaufman, S. L. and Dorman, F. D. (1991a) Method and apparatus for determining concentration of macromolecules and colloids in a liquid sample. *U.S. Patent*, 5076097.
Zarrin, F., Kaufman, S. L. and Socha, J. R. (1991b) Droplet size measurement of various nebulizer using differential electrical mobility particle sizer. *J. Aerosol Sci.* **22,** S343–346.
Zeleny, J. (1915) On the conditions of instability of liquid drops, with applications to the electrical discharge from liquid point. *Proc. Camb. Phil. Soc.* **18,** 71–83.